Spatial modeling of long-term air temperatures for sustainability: Evolutionary fuzzy approach and neuro-fuzzy methods

6 Aboalghasem Sadeghi-Niaraki[1,2*], Ozgur Kisi[3], Soo-Mi Choi[2]

7 [1]Geoinformation Tech. Center of Excellence, Faculty of Geomatics, K.N.Toosi University of Technology, Tehran,
8 Iran
9 [2]Department of Computer Science and Engineering, Sejong University, Seoul, Republic of Korea
10 [3]Faculty of Natural Sciences and Engineering, Ilia State University, Tbilisi, 0132, Georgia
11
12   *Correspondence: a.sadeghi.ni@gmail.com

Abstract.

16 This paper investigates the capabilities of the evolutionary fuzzy genetic (FG) approach and

17 compares it with three neuro-fuzzy methods—neuro-fuzzy with grid partitioning (ANFIS-GP),

18 neuro-fuzzy with subtractive clustering (ANFIS-SC), and neuro-fuzzy with fuzzy c-means

19 clustering (ANFIS-FCM)—in terms of modeling long-term air temperatures for sustainability

20 based on geographical information. In this regard, to estimate long-term air temperatures for a 40-

21 year (1970–2011) period, the models were developed using data for the month of the year, latitude,

22 longitude, and altitude obtained from 71 stations in Turkey. The models were evaluated with

23 respect to mean absolute error (MAE), root mean square error (RMSE), Nash–Sutcliffe efficiency

24 (NSE), and the determination coefficient ($R2$). All data were divided into three parts and every

25 model was tested on each. The FG approach outperformed the other models, enhancing the MAE,

26 RMSE, NSE, and $R2$ of the ANFIS-GP model, which yielded the highest accuracy among the

27 neuro-fuzzy models by 20%, 30%, and 4%, respectively. A geographical information system was

28 used to obtain temperature maps using estimates of the optimal models, and the results of the

29 model were assessed using it.

31 **Keywords:** Long-term air temperature; estimation, evolutionary fuzzy; neuro-fuzzy; GIS.

1 Introduction

33 Regional climate is critical to the efficiency of crops as it deeply influences their yield potential.

34 Rainfall, solar irradiance, and the temperature of the air are factors affecting crop yield,

35 improvement, and growth (Ali-Nezhad and Eskandari, 2012). With regard to the phonological

36 levels of the ripening of a crop, temperature is considered vital. (Rosenzweig and Liverman, 1992).

37 Moreover, crop growth is done within only specific temperature ranges. While the growth of a

38 plant relies heavily on temperature, the plant species is the most significant determinant of the

39 range of temperature ideal for its growth (Hasanuzzaman et al., 2013). Temperature determines

40 the crop's survival and growth in each region (Cobaner et al. 2014). Brunetti et al. (2014) discuss

41 the pros and cons of 3 spatial models such as multi-linear regression with local improvements

42 (MLRLI), regression kriging (RK), local weighted linear regression (LWLR) considering

43 elevation input for temperature assessment in Italy. Hidalgo et al. (2015) employ spatial trend

44 analysis based on the interpolation method such as radial weight with a Gaussian shape using

45 angular weight for temperature data analysis. Serrano-Notivoli et al. (2019) evaluate spatial,

46 temporal variability of temperature using methods such as Generalized Linear Mixed (GLMM)

47 and Generalized Linear Models (GLM) with the inclusion of spatial predictors such as latitude,

48 longitude, altitude, and distance.

49 Techniques from artificial intelligence (AI), such as the adaptive neuro-fuzzy inference system

50 (ANFIS) and artificial neural networks (ANN), have been used in such subjects as agro-hydrology,

51 agro-meteorology, and engineering for water resources. This study focuses on the relevant

52 literature. Zhu et al. (2019) proposed a model using different machine learning techniques such

53 as multilayer perceptron neural network models (MLPNN), adaptive neuro-fuzzy inference

54 systems (ANFIS) with fuzzy c-mean clustering algorithm (ANFIS_FC), ANFIS with grid partition

55 method (ANFIS_GP), and ANFIS with subtractive clustering method (ANFIS_SC) for prediction

56 of water temperature. Khosravi et al. (2018) employs a model using multilayer feed-forward neural

57 network (MLFFNN), radial basis function neural network (RBFNN), support vector regression

58 (SVR), fuzzy inference system (FIS) and adaptive neuro-fuzzy inference system (ANFIS) for solar

59 radiation prediction.

60 The abductive neural network method was utilized by Abdel-Aal to predict air temperature every

61 hour. Using data concerning seasonality and changing the parameters of an ANN model, Smith et

62 al. (2005) developed an ANN for temperature forecasting. Dew-point temperature was modeled

63   by Shank et al. (2008) using neural networks, and Turkey's long-term temperature forecasting was

64   applied by Bilgili and Sahin (2009) to each month. A new method utilizing the Yule–Walker

65   equation and ANNs was proposed by Chattopadhyay et al. (2011) to model the time series of

66   monthly maximum temperatures in northeast India. Turkey's mean air temperature for each month

67   was modeled by Sahin (2012) using ANN and remote sensing. By using geographical data, the

68   performance of ANNs and ANFIS was compared in terms of forecasting air temperature in Iran

69   by Kisi and Shiri. In another study, the monthly mean of Turkey's air temperature was predicted

70   by Cobaner et al. (2014) using ANNs and ANFIS. All past assessments have used ANFIS and

71   ANNs, and none of them has evaluated fuzzy methods for long-term modeling of temperature by

72   applying geographical information. Thus, this paper aims to model long-term temperatures using

73   geographical data and compare an evolutionary fuzzy method with three approaches based on

74   ANFIS.

75   Some researchers in climatology, biogeography, hydrology, meteorological, agriculture, and

76   ecology have applied temperature modeling using spatial/geographical information systems (GIS)

77   (Ninyerola et al., 2000). Goodale et al. (1998) applied predictors to interpolate temperature and

78   precipitation in Ireland using spatial information (latitude, longitude, and altitude). Geostatistical

79   model kriging was employed by Benavides et al. (2007) to model temperature. Chuanyan et al.

80   (2005) compared the results of conventional predictive models, such as linear regression and

81   geostatistical interpolation techniques (e.g., ordinary kriging, splines, and inverse distance weight),

82   in terms of spatial distribution in modeling surface air temperature. Ninyerola et al. (2000) also

83   employed GIS-based techniques for the accurate prediction and mapping of the nonlinear behavior

84   of air temperature over space and time.

85   To predict long-term monthly air temperature with spatial data for achieving sustainability, in this

86   research the evolutionary fuzzy genetic (FG) model applicability is examined. The results of the

87   proposed model were evaluated by comparing with those of three ANFIS models: ANFIS using

88   fuzzy c-means clustering (ANFIS-FCM), ANFIS using grid partitioning (ANFIS-GP), and ANFIS

89   using subtractive clustering (ANFIS-SC). In this regard, training and testing the FG and ANFIS

90   models were conducted on 71 weather stations data in Turkey. The results were also evaluated

91   using the GIS method.

2 Study area

The 37th largest country in the world, Turkey is located at 38.9637° N latitude and 35.2433° E longitude with an area of 780,000 km², 25 million hectares of which is suited for agriculture. Turkey is a mountainous country with large plains. The highest mountain, Ararat, is 5165 meters high. The distribution of temperature and weather patterns are significantly influenced by the orientation and elevation of mountains in the country.

This study used monthly mean temperatures gathered from 71 stations of the Turkish State Meteorological Service. This information included a 40-year dataset from 1970–2011 for each station. Table 1 shows the temperature (°C), longitude, latitude, and altitude above sea level as recorded by each station. The temperature varied from -11.5 °C in January (Ardahan) to 32 °C in July (Urfa) in the long term. The high variation may have occurred because of the sea rounding these areas, the high mountains along the coasts of the Black Sea and the Mediterranean Sea, and the mountainous eastern Anatolia region (Cobaner et al., 2014). Figure 1 shows the meteorological stations distribution in Turkey.

3 Methods

3.1 Fuzzy approach

Fuzzy logic has been used in such fields as business, engineering, and the sciences (Zadeh, 1965). Figure 2 shows units of fuzzification of a general fuzzy system including a fuzzy inference engine, a fuzzy rule base, and defuzzification. Fuzzy logic is based on the idea of using hybrid systems, where part of one system and part of another are used instead of only one. The degree of dependence on a system is a number between zero and one.

In the inference mode, the fuzzy system takes inputs and outputs data. By using a map of association, namely fuzzy associative memory, the inputs are transformed into the equivalent output sets by fuzzy system learning (Kosko, 1993). Some "black box" approaches such as ANNs can function, for example, in regression, but fuzzy systems are clearer and more pliable. Thus, it is clear how fuzzy systems perform and modify processes (Russel & Campbell, 1996).

120   The fuzzy method used here is as follows. Several subsets using Gaussian member function

121   are formed from the input and output parameters. ck fuzzy rules are available, where c and k are

122   the subsets and inputs numbers, respectively. Efficiency increases with the number of subsets, and

123   the rule base increases in weight, rendering construction more complex. In the case of only one

124   input, x, and k subsets, the rule base yields yn (n=1, 2, …, k2) (Şen, 1998).

125   In the case of one variable input, x with four values of "low," "medium," "high," and "very

126   high," four rules are possible:

127   R1: IF x is "low," THEN y_1

128   R2: IF x is "medium," THEN y_2

129   R3: IF x is "high," THEN y_3

130   R4: IF x is "very high," THEN y_4

131   The output is single weighted, y, as a weighted average of the outputs of these four rules as follows:

132       $$y = \frac{\sum_{n=1}^{4} w_n \cdot y_n}{\sum_{n=1}^{4} w_n}$$ (1)

133   where the degree of membership, w_n, is investigated for each x to be assigned an equivalent y_n

134   after triggering each rule.

135   Therefore, having formed the rule base, any assortments of subsets of the parameters used as

136   input to the fuzzy system, Eq. (1), can be used to compute the output values (y) (Şen, 1998).

137   The proposed fuzzy base rule can be computed using the datasets used as input and output

138   as follows:

139   1.   using the smallest number of inputs;

140   2.   assigning a specific membership function to each input;

141   3.   computing the value of membership (w_n) of x in all fuzzy subsets;

142   4.   calculating the output y_n simultaneously with the weight set w_n;

143   5.   renewing all other data points; and

144   6.   calculating the weighted average using Eq. (1) (Kiszka et al., 1985a; Kiszka et al., 1985b).

145   As any change in the subsets makes a direct effect on the functionality of the fuzzy model, forming

146   the fuzzy subsets is among the most challenging problems in the area. It is thus vital to define the

147   membership functions optimally to maximize modeling efficiency (Kisi and Cengiz, 2013). The

148   optimal membership functions are defined in this research using the genetic algorithm.

3.2 Genetic algorithm

GAs have been researched in engineering since 1960, when they were introduced by Holland (Abraham et al., 2005; Ortiz et al., 2004). In general, GAs try to imitate the Darwinian concept of natural selection. A GA first generates a set of possible solutions and tries to find the best approach to survival to form a new population of solutions, which assesses the real solution better than before. The challenge of creating better and fitter solution sets is the basic principle of GAs. They are utilized to find the best and most optimal solutions to solve difficult problems. Utilizing this approach provides a useful option for solutions (Aijun et al., 2004; Tsai et al., 2004). While other methods are restricted due to their suppositions, GAs have fewer such limits (Jean et al., 2007).

3.3 Adaptive neuro-fuzzy inference system

ANFIS, a general investigation tool with the quality to approximate continuous real functions on compact sets, was developed in 1993 by Jang. In its structure, nodes are attached to one another by directional links. A node function containing variable or constant parameters introduces the node (Jang et al., 1997).

The example below presents a typical fuzzy inference system (FIS) with an output f, three inputs x, y, and z, and two if–then fuzzy rules of the Takagi and Sugeno type:

Rule 1: If x is A1, y is B1, and z is C1, then $f_1 = p_1 x + q_1 y + r_1 z + s_1$ (2)

Rule 2: If x is A2, y is B2, and z is C2, then $f_2 = p_2 x + q_2 y + r_2 z + s_2$ (3)

where f_1 and f_2 are the output functions of rules 1 and 2, respectively. Figure 3 shows the structure of ANFIS. The functions of the nodes are as follows.

$O_{1,i} = \varphi A_i(x)$ indicates the node function for each square node i of layer 1 that is adaptive, and i = 1, 2, x, is the ith input node; A_i is a linguistic label (i.e., "small" or "big") for this node function. When input x satisfies quantifier A_i, $O_{1,i}$, is the membership function (MF) of fuzzy set A (e.g., A_1, A_2, B_1, B_2, C_1, C_2) and indicates its degree. $\varphi A_i(x)$ is mainly a Gaussian function ranging between zero and one as the minimum and maximum levels, respectively:

$$\varphi A_i(x) = \exp(-\left(\frac{x - a_i}{b_i}\right)^2)$$ (4)

177

178 where $\{a_i, b_i\}$ is the parameter set. These layer parameters are considered to be assumed. The circle

179 nodes of layer 2 have index Π, which indicates the multiplication of the inputs and the sending of

180 the product. For instance, $w_i = \varphi A_i(x)\varphi B_i(y)\varphi C_i(z)$, i = 1, 2. The output of each node shows the

181 impression level of a rule. Circle nodes of layer 3 take the label N. Following this, the ratio of the

182 level of impression of the ith rule on the sum of the levels of all rules is computed by the ith node

183 using

184 $$\overline{w}_i = \frac{w_i}{w_1 + w_2}, \quad i = 1, 2. \tag{5}$$

185 The node function of the square nodes of layer 4 is $O_{4,i} = \overline{w}_i f_i = \overline{w}_i (p_i x + q_i y + r_i z + s_i)$, where

186 $\overline{w}_i$ represents the layer 3 output and the parameter series is $\{p_i, q_i, r_i, s_i\}$. These layer parameters

187 are called consequent parameters. The single circle nodes of layer 5, labeled "Σ," sums all

188 incoming signals and returns the result as the final output:

189 $$O_{5,i} = \sum_{i=1} \overline{w}_i f_i = \frac{\sum_i w_i f_i}{\sum_i w_i} \tag{6}$$

190 The ANFIS network acts similarly to a first-order Sugeno FIS (Kisi, 2015). Linear or fixed-valued

191 functions are used in ANFIS to generate the output. Detailed information concerning ANFIS is

192 available in Jang's study (1993).

3.4 Grid partitioning

194 This approach provides independent partitions of prior variables (Jang, 1993). The membership

195 functions of all prior variables can be determined by prior knowledge and experience. Expressing

196 the meaning of the linguistic terms of a context is the goal of designing these partitions. However,

197 in many systems, there is no specific information accessible to these partitions. Thus, the ranges

198 of the prior variables may easily be divided into membership functions that are equally shaped and

199 spaced. The membership functions may be located suitably in case the system's input–output data

200 are available. The rule base should be generated in a manner that perfectly covers previous fuzzy

201 set combinations. The membership functions of each variable are built apart from those of others,

202   and this is the main disadvantage of this method as this causes it to overlook the relationship among

203   variables (Vernieuwe et al. ,2005).

3.5 Subtractive clustering

205   The ANFIS subtractive clustering (ANFIS-SC) model is defined by merging ANFIS with

206   subtractive clustering. In this model, a possible cluster center is each data point, which is not a grid

207   point (Chiu, 1994). It is thus an extended model of Yager and Filev (1994), the mountain clustering

208   method.

209   In this approach, the number of effective "grid points" that should be investigated are similar to

210   the number of data points independently of the number of dimensions of the problem. One of the

211   advantages of this approach is that a tradeoff between computational complexity and accuracy is

212   unnecessary because the need to define a grid resolution is removed. The scale of the mountain

213   method to accept or reject the cluster centers is also extended in subtractive clustering.

214   The impressive radius is vital to defining the number of clusters. Too many smaller clusters require

215   more rules if a small radius is chosen, and vice versa. Thus, selecting a suitable impressive radius

216   for data space clustering is crucial. Defining the number of fuzzy rules and presumptions of the

217   fuzzy MF is the next stage. In the end, the results in the output MF are generated by utilizing linear

218   least squares, which builds a valid FIS (Cobaner, 2011; Sanikhani and Kisi, 2012).

3.6 Fuzzy c-means clustering

220   C-means fuzzy clustering is a form of flexible clustering model in which the data points are

221   combined by calculating possible data points in the feature space. In this model, the mountain

222   clustering approach can be used to calculate the number of clusters and cluster centers (Chiu, 1994;

223   Cobaner, 2011). This model is based on the k-means algorithm, which is unsuitable for big

224   datasets. C-means fuzzy clustering reduces the intra-cluster variance to a minimum (Ayvaz et al.,

225   2007) and combines data using its clustering algorithm. The c-means fuzzy clustering minimizes

226   either the distance or the objective squared error function (Kisi, 2015).

3.7 Spatio–temporal modeling

228   The use of GIS for the spatial modeling of many real-world phenomena toward implementation

229   for sustainability (Childers et al., 2015; Lundgren and Kjellstrom, 2013) has attracted research

230 attention. Spatial modelling acts like a critical tool to examine the nature or property of real-world
231 phenomena whether being sustained or not. Much of real-world phenomena are dynamic, and
232 involve spatial and temporal changes. Thus, the use of a GIS for temporal and spatial modeling
233 plays an important role in improving model visualization and tracking how much far from
234 sustainability indicators (Figure 4). The GIS is used for various purposes, such as creating the
235 required spatial data (geographical location) used as input for the prediction model. Using the
236 spatial functions generates a map related to the modeling phenomena to assess their behavior and
237 at different locations. Such spatial statistical functions as zonal statistics assess variation in
238 phenomena as well as minimum and maximum mean values at different locations. A geospatial
239 function, such as the interpolation method, enables the elimination of possible model defects (e.g.,
240 data loss in some areas). Geostatistical analysis, such as trend analysis functions, provides
241 forecasting trends and patterns of phenomena.

242 ## 3.8 Model evaluation statistics

243 Four statistics were used to evaluate the models: mean absolute error (MAE), root mean square
244 error (RMSE), Nash–Sutcliffe efficiency (NSE), and the determination coefficient (R^2). RMSE,
245 MAE, and NSE can be expressed as

246
$$RMSE = \sqrt{\frac{1}{n}\sum_{i=1}^{n}\left(AT_{M,i} - AT_{o,i}\right)^2} \tag{7}$$

247
$$MAE = \frac{1}{n}\sum_{i=1}^{n}\left|AT_{M,i} - AT_{o,i}\right| \tag{8}$$

248
$$NSE = 1 - \frac{\sum_{i=1}^{n}(AT_{M,i} - AT_{o,i})}{\sum_{i=1}^{n}(AT_{o,i} - \overline{AT_o})} \tag{9}$$

249 where AT_M and AT_o are modeled and observed air temperatures, respectively, n is the number of
250 time steps, and $\overline{AT_o}$ is the mean observed air temperature.

251 **4. Application and Results**

252 **4.1 Modeling long-term air temperatures using evolutionary fuzzy and neuro-**
253 **fuzzy approaches**

254 Four hybrid fuzzy methods—evolutionary FG, ANFIS-GP, ANFIS-SC, and ANFIS-FCM—were
255 compared in terms of predicting long-term air temperatures. The inputs of the models were
256 latitude, longitude, altitude and month of the year. To train and test models, the data of 71 weather
257 stations in Turkey were used. The entire dataset (the 70 stations × 12 months = 840 data items)
258 was divided into three subsets. The first 23 stations were used in the first part, the second set of 23
259 for the second, and the other 24 stations were used for the last part. In the first application, training
260 and testing were conducted using the first two parts (subsets) and the third part respectively; it was
261 called model 1 (M1). In the second application, training was conducted using the second and third
262 parts and testing was conducted using the first part, and was called model 2 (M2). In the last
263 application, training was conducted using the first and third parts the testing was conducted using
264 the second part, and was called model 3 (M3).

265 ANFIS-GP was applied to the datasets, and two and three Gaussian membership functions (MFs)
266 were used to find the optimal one. More than three MFs led to worse results and memory-related
267 problems. The number of iterations was varied from 10 to 100 with increments of 10 for each
268 number of MFs. Different values of the radius were used (from 0.1 to 1 in increments of 0.1) for
269 the ANFIS-SC model, and different numbers of clusters were used (from two to eight, incremented
270 by one) for the ANFIS-FCM model. The numbers of iterations used were similar to those in the
271 ANFIS-GP and ANFIS-SC methods. To test the FG models, the optimal number of MFs for the
272 ANFIS-GP models were used. A total of 1,000 iterations and 100 members were used for the FG
273 models. The optimal parameters and structures of the applied models are listed in Table 2. For
274 example, 3-3-2-3,100 indicates an ANFIS-GP model with three, three, two, and three MFs for the
275 four inputs (month of the year, latitude, longitude, and altitude) over 100 iterations. The number
276 1,100 indicates the value of the radii and the number of iterations of the ANFIS-SC model, the
277 numbers of clusters and iterations of the ANFIS-FCM model were 5,100. "3-3-2-3, 1000, 100,"
278 indicating an FG model with three, three, two, and three MFs for the four inputs with 1,000
279 generations and a population of 100.

280 Table 3 specifies the results of training and testing the models in terms of RMSE, MAE, NSE, and
281 R^2. In the training stage, the RMSE of the FG model ranged from 1.59 to 1.89, whereas that of

282 ANFIS-GP, ANFIS-SC, and ANFIS-FCM was in the range 2.16–2.95, 1.14–1.45, and 6.13–6.93,

283 respectively. Similar ranges were observed for the MAE, NSE, and R^2. The ranges and means

284 reveal that the ANFIS-SC was the most accurate in terms of approximating long-term air

285 temperatures followed by the FG. ANFIS-FCM yielded the worst results in this stage. In the test

286 stage, however, the ranges of RMSE, MAE, NSE, and R^2 of the FG models were 1.63–3.26, 1.23–

287 2.08, 0.868–0.967, and 0.882–0.967, respectively, which were superior to the those of the other

288 models. The average RMSE, MAE, NSE, and R^2 of the optimal FG models (2.32, 1.59, 0.925, and

289 0.935) were also higher than those of the ANFIS-GP (2.91, 2.28, 0.890, 0.898), ANFIS-SC (5.41,

290 3.42, 0.539, 0.768), and ANFIS-FCM (12.5, 8.32, 0.239, 0.250) models. Among the neuro-fuzzy

291 models, ANFIS-GP obtained the highest accuracy. In terms of RMSE, MAE, NSE, and R^2, the FG

292 model enhanced the accuracy of ANFIS-GP by 20%, 30%, 4%, and 4%, respectively.

293 A graphical comparison of the four methods is provided in Figures 5–7 for M1, M2, and M3. The

294 obvious finding from Figure 4 is that the estimates of the FG model were closer to the

295 corresponding observed temperatures than those of the ANFIS-GP, ANFIS-SC, and ANFIS-FCM

296 models. Considerable under/over-estimations were observed in the ANFIS-FCM model. The

297 scatterplots show that the fit line equation of the FG model was y = 0.9910x–0.906, closer to the

298 exact line (y=x) with a higher R^2 than the other three models. ANFIS-GP was better than the other

299 two neuro-fuzzy models. Similar trends were seen for M2 and M3 (see Figures 6–7).

300

301 ## 4.2 Spatial modeling of long-term air temperatures using GIS

302 Air temperature is a spatio-temporal phenomenon, and thus changes with time and place. Based

303 on their capabilities, GIS spatial functions can be used to improve the model. The GIS can be

304 used to provide additional input for air temperature modeling in the form of spatial data (latitude

305 and longitude). This spatial modeling leads to greater flexibility in the proposed model and

306 renders it more adaptable for practical use. Moreover, the GIS is used to create temperature map-

307 related locations to enable better visualization and interpretation of the outputs.

308 A classified temperature mapping enables a comparison of the variation in temperature ranges of

309 all methods with respect to M1 (Figure 8), M2 (Figure 9), and M3 (Figure 10). The lowest

310 temperature ranges according to the classified temperature map in M1 were ANFIS-SC: 4.52–

311 8.74, ANFIS-FCM: 6.14–8.95, ANFIS-GP: 8.45–10.22, and FG-FUZZY-G: 8.94–10.47. The

312   maximum temperatures were ANFIS-SC: 18.82–22.75, ANFIS-FCM: 17.45–20.21, ANFIS-GP:

313   16.02–18.05, and FG-FUZZY-G: 16.75–18.47. The lowest temperatures ranges according to M2

314   were ANFIS-SC: -5.09– -3.33, ANFIS-FCM: -85.50– -6, ANFIS-GP: 7.22–9.34, and FG-

315   FUZZY-G: 4.46–7.62, and the maximum temperatures were ANFIS-SC: 37.08– -48.67, ANFIS-

316   FCM: 13.38–24.13, ANFIS-GP: 16.35– 18.47, and FG-FUZZY-G: 15.21–17.51. The lowest

317   temperature ranges in M3 were ANFIS-SC: 8.15–10.75, ANFIS-FCM: 4.60–9.20, ANFIS-GP:

318   10.23–11.75, and FG-FUZZY-G: 7.96–10.29), and the maximum temperatures were ANFIS-SC:

319   18.08–19.98, ANFIS-FCM: 23.60–26.73, ANFIS-GP: 17.43–19.23, and FG-FUZZY-G: 16.02–

320   17.48.

321   Furthermore, the temperature map helps experts evaluate the temperature in different locations to

322   identify places with maximum or minimum temperatures. For example, in M1, Osmaniye, in M2,

323   Adana, and in M3, Hatay had the highest temperatures in the best FG method. The unique

324   functionality of other GISs in this section helps address defects in the proposed model.

325   Following this, if there is information loss in some areas, the maps use interpolation functions to

326   yield the temperature.

327   **5. Discussion**

328   As mentioned in the previous section, the ANFIS-GP has memory-related problems when it has

329   much membership functions (more than 3 in this study). In fact, this also changes with respect to

330   input numbers. In this study, 4 inputs were used and, in this case, the use of 4 membership functions

331   causes memory problem. This is due to the fact that ANFIS-GP consider all rules combinations,

332   and it therefore has much more premise parameters, which show the membership functions' shape

333   and location and consequent parameters that compose the equations of considered rules. However,

334   the main advantage of this method is that it is more flexible because of high number of weights

335   compared to other ANFIS methods, ANFIS-SC and ANFIS-FCM. The main advantages of the

336   ANFIS-SC and ANFIS-FCM methods are the use of less parameters or weights because they use

337   clustering algorithms, and they can therefore optimize rule or membership functions' numbers.

338   However, this property may cause inappropriate learning of these methods compared to ANFIS-

339   GP.

340   The FG model was found to be the best method in modelling long-term temperatures, followed by

341   the ANFIS-GP method. The FG also uses all rules combinations similar to ANFIS-GP and

342   therefore, it has much more premise parameters which show the membership functions' shape and

343   location and consequent parameters. The main advantage of the FG due to its evolutionary training

344   algorithm (genetic algorithm, GA). In ANFIS-GP, gradient descent (GD) algorithm is utilized for

345   the optimization of membership functions' parameters (premise parameters). The GD can be

346   trapped into local optima, while this does not occur for the GA algorithm.

347

6. Conclusions

349   In this paper, the capabilities of evolutionary fuzzy genetics were compared with three neuro-fuzzy

350   techniques in terms of estimating long-term air temperatures for sustainability. Data from 71

351   stations from Turkey were used and divided into three equal parts. The applied models were tested

352   using each part. Each method was hence tested three times with all the data. Finally, a GIS was

353   used to produce air temperature maps based on the results of the optimal models. Three main

354   results can be drawn from the application:

355   i-   The evolutionary FG model is superior to the ANFIS-GP, ANFIS-SC, and ANFIS-

356   FCM at modeling long-term air temperatures.

357   ii-   Of the neuro-fuzzy methods, the ANFIS-GP outperformed the ANFIS-SC and ANFIS-

358   FCM.

359   iii-   The accuracy of the best neuro-fuzzy model, the ANFIS-GP, in terms of RMSE, MAE,

360   NSE and R^2 increased by 20%, 30%, 4%, and 4%, respectively, using the FG model.

361

Funding

363   This research was supported by the MSIT (Ministry of Science and ICT), Korea, under the ITRC

364   (Information Technology Research Center) support program (IITP-2019-2016-0-00312).

365   **References**

366   Abdel-Aal, R.E.: Hourly temperature forecasting using abductive networks. Engineering Applications of Artificial

367   Intelligence, 17(5):543-556, 2004.

368   Abraham, A. and Jain, L.: Evolutionary Multiobjective Optimization: Theoretical Advances and Applications,
369   Springer, London, 1-6 pp., 2005.

370   Aijun, L., Hejun, L., Kezhi, L. and Zhengbing, G.: Applications of neural networks and genetic algorithms to CVI
371   processes in carbon/carbon composites. Acta Mater, 52(2):299-305, 2004.

372   Ali-Nezhad, F.M. and Eskandari, H.: Effect of architectural design of greenhouse on solar radiation interception and
373   crops growth conditions. Int. J. Agric. Crop Sci., 4(3):122-127, 2012.

374   Ayvaz, M.T., Karahan, H. and Aral, M.M.: Aquifer parameter and zone structure estimation using kernel-based fuzzy
375   c-means clustering and genetic algorithm. J Hydrol, 343(3-4):240-253, 2007.

376   Benavides, R., Montes, F., Rubio, A. and Osoro, K.: Geostatistical modelling of air temperature in a mountainous
377   region of Northern Spain. Agricultural and Forest Meteorology, 146(3-4):173-188, 2007.

378   Bilgili, M. and Sahin, B.: Prediction of long-term monthly temperature and rainfall in Turkey. Energy Sources, Part
379   A: Recovery, Utilization, and Environmental Effects, 32(1):60-71, 2009.

380   Chattopadhyay, S., Jhajharia, D. and Chattopadhyay, G.: Univariate modelling of monthly maximum temperature time
381   series over northeast India: neural network versus Yule–Walker equation based approach. Meteorol.
382   Appl., 18(1):70-82, 2011.

383   Brunetti, M. , Maugeri, M. , Nanni, T. , Simolo, C. and Spinoni, J. (2014), High-resolution temperature climatology
384   for Italy: interpolation method intercomparison. Int. J. Climatol., 34: 1278-1296. doi:10.1002/joc.3764

385   Childers, D., Cadenasso, M., Grove, J., Marshall, V., McGrath, B. and Pickett, S.: An ecology for cities: A
386   transformational nexus of design and ecology to advance climate change resilience and urban
387   sustainability. Sustainability, 7(4):3774-3791, 2015.

388   Chiu, S.L.: Fuzzy model identification based on cluster estimation. J Intell Fuzzy Syst, 2(3):267-278, 1994.

389   Chuanyan, Z., Zhongren, N. and Guodong, C.: Methods for modelling of temporal and spatial distribution of air
390   temperature at landscape scale in the southern Qilian mountains, China. Ecological Modelling, 189(1-2):209-220,
391   2005.

392   Cobaner, M.: Evapotranspiration estimation by two different neuro-fuzzy inference systems. J Hydrol, 398(3-4):292-
393   302, 2011.

394   Cobaner, M., Citakoglu, H., Kisi, O. and Haktanir, T.: Estimation of mean monthly air temperatures in
395   Turkey. Computers and Electronics in Agriculture, 109:71-79, 2014.

396   Goodale, C.L., Aber, J.D. and Ollinger, S.V. Mapping monthly precipitation, temperature, and solar radiation for
397   Ireland with polynomial regression and a digital elevation model. Clim. Res., 10(1):35-49, 1998.

398   Gonzalez-Hidalgo, J. C., Peña-Angulo, D. , Brunetti, M. and Cortesi, N. (2015), MOTEDAS: a new monthly
399   temperature database for mainland Spain and the trend in temperature (1951–2010). Int. J. Climatol., 35: 4444-
400   4463. doi:10.1002/joc.4298

401   Hasanuzzaman, M., Nahar, K. and Fujita, M.: Extreme temperature responses, oxidative stress and antioxidant defense
402   in plants. In Abiotic stress-Plant responses and applications in agriculture, ISBN: 978-953-51-1024-8, InTech, doi:
403   http://dx.doi.org/10.5772/54833, 2013.

404 Jang, J.S.: ANFIS: adaptive-network-based fuzzy inference system. IEEE Trans. Syst. Man Cyber., 23(3):665-685,
405   1993.

406 Jang, J.-S.R., Sun, C.-T., and Mizutani, E.: Neuro-Fuzzy and Soft Computing: A Computational Approach to Learning
407   and Machine Intelligence. Prentice Hall, Upper Saddle River, New Jersey, USA,1997.

408 Jean, M.D., Lin, B.T. and Chou, J.H.: Design of a fuzzy logic approach based on genetic algorithms for robust plasma-
409   sprayed zirconia depositions. Acta materialia, 55(6):1985-1997, 2007.

410 Khosravi, A., Koury, R. N. N., Machado, L., & Pabon, J. J. G. (2018). Prediction of hourly solar radiation in Abu
411   Musa Island using machine learning algorithms. Journal of Cleaner Production, 176, 63-75.

412 Kisi, O. and Cengiz, T.M.: Fuzzy genetic approach for estimating reference evapotranspiration of Turkey:
413   Mediterranean region. Water Resour Manage, 27(10):3541-3553, 2013.

414 Kisi, O.: Streamflow forecasting and estimation using least square support vector regression and adaptive neuro-fuzzy
415   embedded fuzzy c-means clustering. Water Resour Manage, 29(14):5109-5127, 2015.

416 Kisi, O. and Shiri, J.: Prediction of long-term monthly air temperature using geographical inputs. Int. J.
417   Climatol., 34(1):179-186, 2014.

418 Kiszka, J. B., Kochanskia, M. E. and Sliwiska, D. S.: The influence of some fuzzy implication operators on the
419   accuracy of fuzzy model, Part I. Fuzzy Set and Syst, 15, 111–128, 1985a.

420 Kiszka, J. B. Kochanska, M. E. and Sliwinska, D. S.: The influence of some fuzzy implication operators on the
421   accuracy of a fuzzy model, Part II. Fuzzy Set and Syst, 15, 223–240, 1985b.

422 Kosko, B. and Toms, M.: Fuzzy thinking: The new science of fuzzy logic, New York: Hyperion, 1-350pp.,1993.

423 Ninyerola, M., Pons, X. and Roure, J.M.: A methodological approach of climatological modelling of air temperature
424   and precipitation through GIS techniques. Int. J. Climatol., 20(14):1823-1841, 2000.

425 Lundgren, K. and Kjellstrom, T.: Sustainability challenges from climate change and air conditioning use in urban
426   areas. Sustainability, 5(7):3116-3128, 2013.

427 Ortiz Jr, F., Simpson, J.R., Pignatiello Jr, J.J. and Heredia-Langner, A.: A genetic algorithm approach to multiple-
428   response optimization. J Quality Eng, 36(4):432-450, 2004.

429 Rosenzweig, C. and Liverman, D.: Predicted effects of climate change on agriculture: A comparison of temperate and
430   tropical regions. Dalam Global Climate Change: Implications, Challenges, and Mitigation Measures. Dalam SK
431   Majumdar (Ed.) The Pennsylvania Academy of Sciences. PA, 342-61 pp., 1992.

432 Russell, S.O. and Campbell, P.F.: Reservoir operating rules with fuzzy programming. J Water Resour Plann Manage
433   ASCE, 122(3):165-170, 1996.

434 Sanikhani, H. and Kisi, O.: River flow estimation and forecasting by using two different adaptive neuro-fuzzy
435   approaches. Water Resour Manage, 26(6):1715-1729, 2012.

436 Şahin, M.: Modelling of air temperature using remote sensing and artificial neural network in Turkey. Adv. Space
437   Res. h, 50(7):973-985, 2012.

438 Şen, Z.: Fuzzy algorithm for estimation of solar irradiation from sunshine duration. Sol. Energy, 63(1):39-49, 1998.

439 Serrano-Notivoli, R., Beguería, S., and De Luis, M.: STEAD: A high-resolution daily gridded temperature dataset for
440   Spain, Earth Syst. Sci. Data Discuss., https://doi.org/10.5194/essd-2019-52, in review, 2019

441   Shank, D.B., Hoogenboom, G. and McClendon, R.W.: Dewpoint temperature prediction using artificial neural
442   networks. Journal of applied meteorology and climatology, 47(6):1757-1769, 2008.

443   Smith, B.A., McClendon, R.W. and Hoogenboom, G.: An Enhanced Artificial Neural Network for Air Temperature
444   Prediction. In IEC (Prague), 7-12 pp., 2005.

445   Toros, H.: Spatio-temporal precipitation change assessments over Turkey. International Journal of
446   Climatology, 32(9):1310-1325, 2012.

447   Tsai, J.T., Liu, T.K. and Chou, J.H.: Hybrid Taguchi-genetic algorithm for global numerical optimization. IEEE Trans
448   Evolut Comput, 8(4):365-377, 2004.

449   Vernieuwe, H., Georgieva, O., De Baets, B., Pauwels, V.R., Verhoest, N.E. and De Troch, F.P.: Comparison of data-
450   driven Takagi–Sugeno models of rainfall–discharge dynamics. Journal of Hydrology, 302(1-4):173-186, 2005.

451   Yager, R.R. and Filev, D.P.: Approximate clustering via the mountain method. IEEE Trans Syst Man
452   Cybern, 24(8):1279-1284, 1994.

453   Zadeh, L.A.: Fuzzy sets. Information and control, 8(3):338-353, 1965.

454   Zhu, S., Heddam, S., Nyarko, E. K., Hadzima-Nyarko, M., Piccolroaz, S., & Wu, S. (2019). Modeling daily water
455   temperature for rivers: comparison between adaptive neuro-fuzzy inference systems and artificial neural networks
456   models. Environmental Science and Pollution Research, 26(1), 402-420.

457

458

459

Table 1

2 **Table 1.** Summary of the geographical information of the studied weather stations (Kisi et al. 2017)

Station	Lat. (ºN)	Long. (ºW)	Alt. (m)	*T(ºC)	Station	Lat. (ºN)	Long. (ºW)	Alt. (m)	*T(ºC)
Adana	37	35.32	27	19.12	K.maras	37.3	40.77	572	16.81
Adiyaman	37.76	38.27	672	17.24	Karabuk	41.2	32.62	259	13.33
Afyon	38.74	30.55	1034	11.28	Karaman	37.17	33.22	1025	11.88
Agri	39.72	43.05	1632	6.18	Kars	40.59	43.08	400	4.81
Aksaray	38.37	34.03	965	12.02	Kastamonu	41.37	33.77	800	9.73
Amasya	40.65	35.83	412	13.63	Kayseri	38.72	35.49	1093	10.44
Ankara	39.97	32.86	891	11.98	Kirikkale	39.84	33.52	748	12.57
Antalya	36.9	30.79	54	18.40	Kirklareli	41.74	27.22	232	13.20
Ardahan	41.11	42.7	1829	3.75	Kirsehir	39.16	34.15	1007	11.35
Artvin	41.18	41.82	628	12.03	Kilis	36.72	37.12	638	17.10
Aydin	37.84	27.84	56	17.63	Konya	37.99	32.56	1031	11.58
Balikesir	39.63	27.92	102	14.55	Kutayha	39.42	29.99	969	10.75
Bartin	41.62	32.35	30	12.63	Malatya	38.35	38.31	948	13.74
Batman	37.89	41.12	540	16.51	Manisa	38.61	37.4	71	16.98
Bayburt	40.25	40.43	1584	6.93	Mardin	37.31	40.73	1040	16.15
Bilecik	40.14	29.97	539	12.50	Mugla	37.29	28.37	646	15.01
Bingol	38.88	40.49	11.77	11.95	Mus	38.74	41.49	1320	9.71
Bitlis	38.39	42.12	1573	9.53	Nigde	37.97	34.69	1211	11.08
Bolu	40.74	31.6	743	10.53	Osmaniye	37.1	36.25	94	18.24
Burdur	37.72	30.29	967	13.18	Rize	41.04	40.5	9	14.23
Bursa	40.23	29.01	100	14.56	Sakarya	40.77	30.39	31	14.44
Canakkale	40.15	26.41	6	15.01	Samsun	41.35	36.24	4	14.38
Cankiri	40.61	33.61	751	11.18	Siirt	37.93	41.94	896	16.11
Corum	40.54	34.94	776	10.57	Sinop	42.02	35.15	32	14.09
Denizli	37.76	29.09	425	16.21	Sivas	39.74	37.02	1285	9.08
Elazig	38.67	39.22	990	13.03	S.urfa	37.16	38.79	549	18.38
Erzincan	39.74	39.5	1218	10.89	Sirnak	37.52	42.45	1350	14.13
Erzurum	39.95	41.17	17.58	5.40	Tekirdag	40.99	27.49	3	13.96
Eskisehir	39.78	30.58	786	10.84	Tokat	40.3	36.56	608	12.48
Gaziantep	37.07	37.39	855	15.07	Trabzon	41	39.78	39	14.68
Giresun	40.92	38.39	37	14.53	Tunceli	39.1	39.55	978	12.83
Gumushane	40.46	39.47	1219	9.55	Usak	38.67	29.4	919	12.51
Hakkari	37.57	43.75	1728	10.26	Van	38.49	43.39	1661	9.24
Hatay	36.36	36.28	82	18.26	Yalova	40.66	29.27	4	14.67
Igdir	39.92	44.06	858	12.08	Yozgat	39.82	34.81	1298	8.97
Istanbul	40.98	28.82	33	15.01					

3 * T(ºC): average air temperature during the study period

Table 2

2   **Table 2.** Optimal parameters and structures of the ANFIS-GP, ANFIS-SC, ANFIS-FCM and FG models

Model	ANFIS-GP	ANFIS-SC	ANFIS-FCM	FG
M1	3-3-2-3, 100	1, 100	5, 100	3-3-2-3, 1000, 100
M2	3-2-2-2, 100	1, 100	8, 90	3-2-2-2, 1000, 100
M3	3-3-2-3, 100	1, 100	7, 100	3-3-2-3, 1000, 100

Table 3

Table 3. Training and testing results of the FG, ANFIS-GP, ANFIS-SC and ANFIS-FCM models

Process	Model	FG				ANFIS-GP				ANFIS-SC				ANFIS-FCM			
		RMSE (°C)	MAE (°C)	NSE	R²	RMSE (°C)	MAE (°C)	NSE	R²	RMSE (°C)	MAE (°C)	NSE	R²	RMSE (°C)	MAE (°C)	NSE	R²
Training	M1	1.89	1.31	0.955	0.956	2.47	1.98	0.924	0.924	1.24	0.95	0.981	0.981	6.66	5.48	0.448	0.448
	M2	2.19	1.43	0.937	0.938	2.95	2.26	0.886	0.886	1.45	1.10	0.972	0.972	6.93	5.81	0.373	0.373
	M3	1.59	1.25	0.967	0.967	2.16	1.83	0.938	0.938	1.14	0.87	0.983	0.983	6.13	5.06	0.504	0.504
	Mean	1.89	1.33	0.953	0.954	2.53	2.02	0.916	0.916	1.28	0.973	0.979	0.979	6.57	5.45	0.442	0.442
Testing	M1	2.08	1.45	0.940	0.955	2.74	2.26	0.896	0.904	3.93	2.52	0.78	0.820	7.53	6.17	0.209	0.253
	M2	1.63	1.23	0.967	0.967	2.68	2.10	0.910	0.912	9.09	5.64	-0.036	0.602	22.3	12.5	-5.22	0.119
	M3	3.26	2.08	0.868	0.882	3.31	2.47	0.864	0.878	3.21	2.09	0.872	0.882	7.67	6.30	0.269	0.379
	Mean	2.32	1.59	0.925	0.935	2.91	2.28	0.890	0.898	5.41	3.42	0.539	0.768	12.5	8.32	0.239	0.250

Figure 1

Figure 1

Meteorological stations distribution in Turkey (the map was provided by the State State

Hydraulic Works (DSI), see http://en.dsi.gov.tr/about-dsi-)

Figure 2

Figure 2

A typical fuzzy inference system
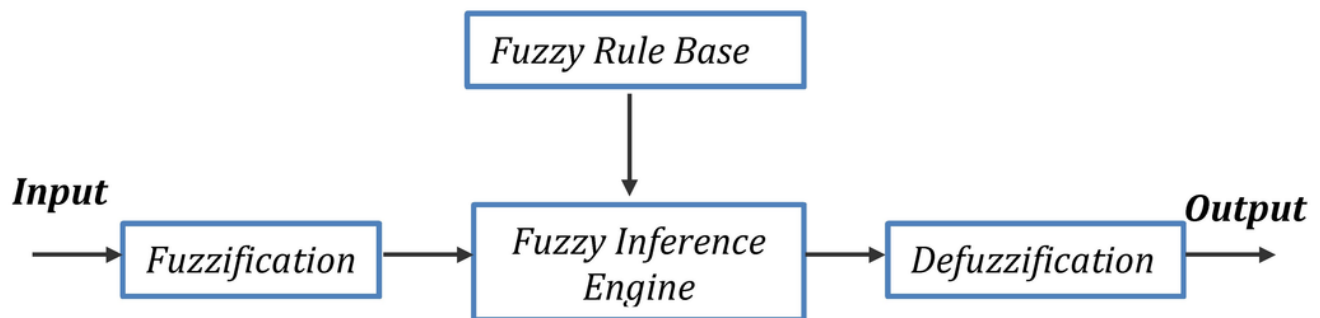
Figure 3

Figure 3

ANFIS model for temperature prediction
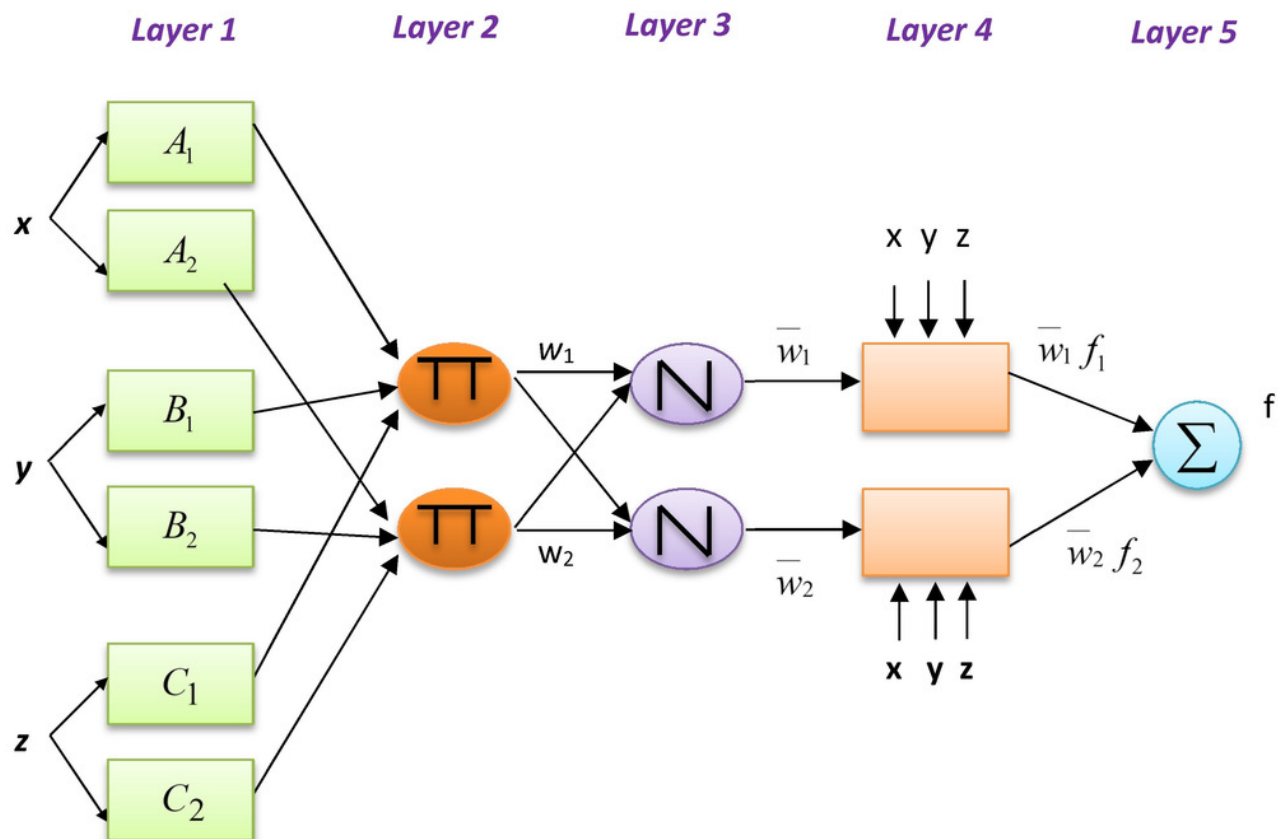
Figure 4

Figure 4

Spatial temporal modeling
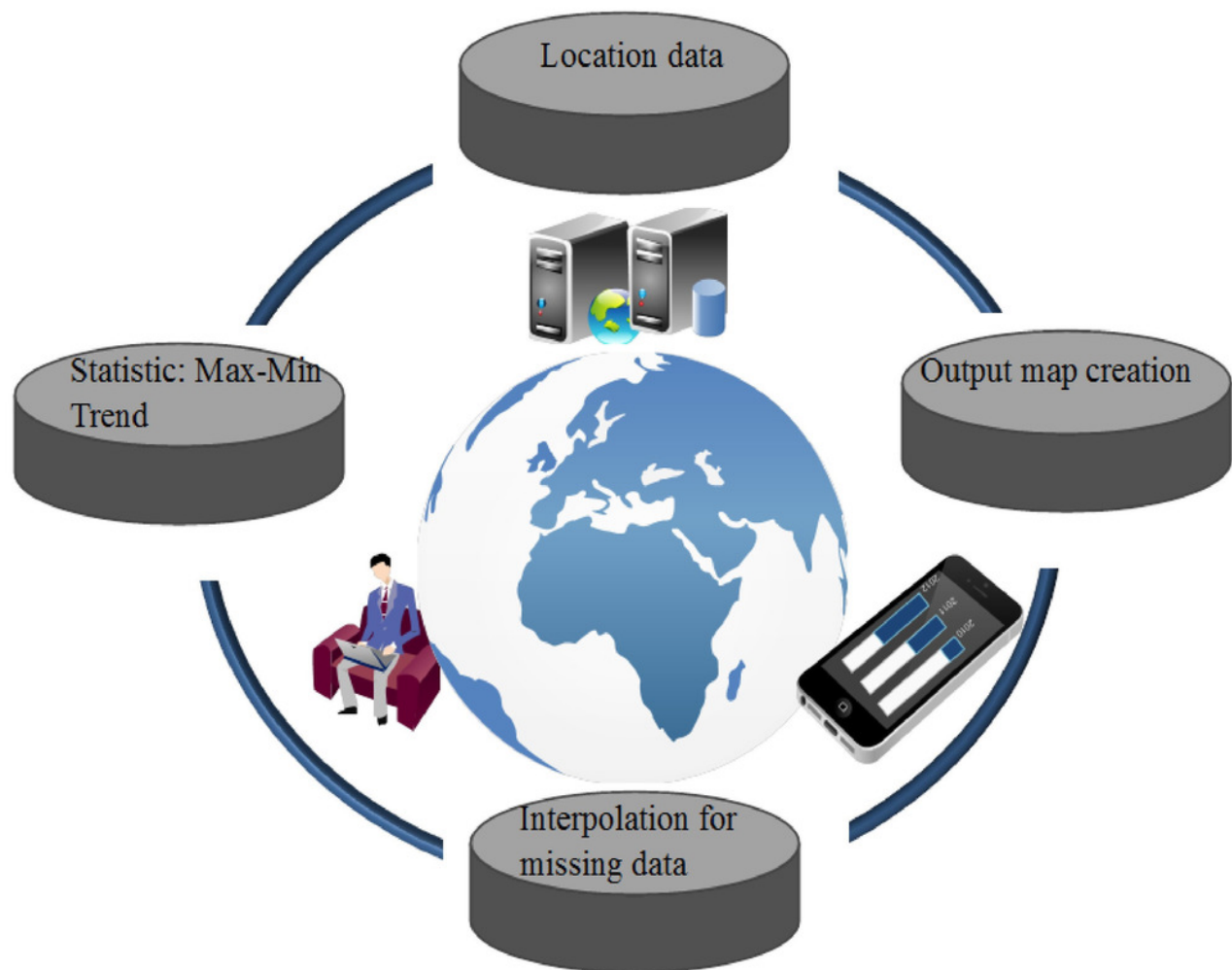
Figure 5

Figure 5.

Observed and predicted air temperatures by FG, ANFIS-GP, ANFIS-SC and ANFIS-FCM models
– M1 models; time variation graphs of (a) FG, (b) ANFIS-GP, (c) ANFIS-SC and (d) ANFIS-FCM
and scatterplots of (e) FG, (f) ANFIS-GP, (g) ANFIS-SC and (h) ANFIS-FCM
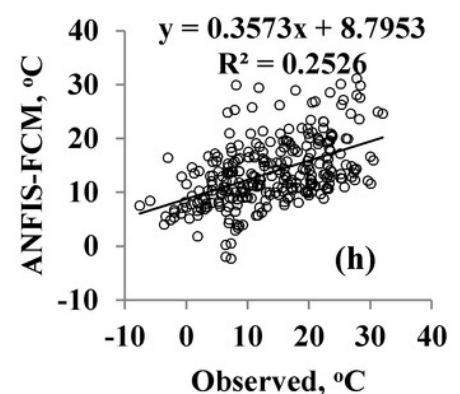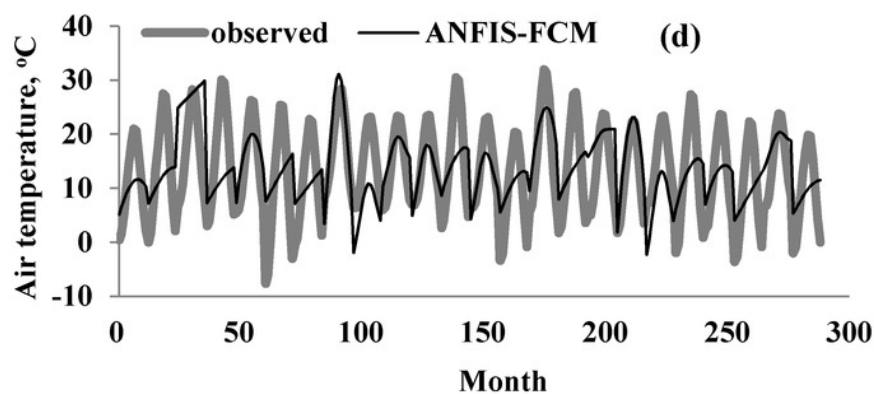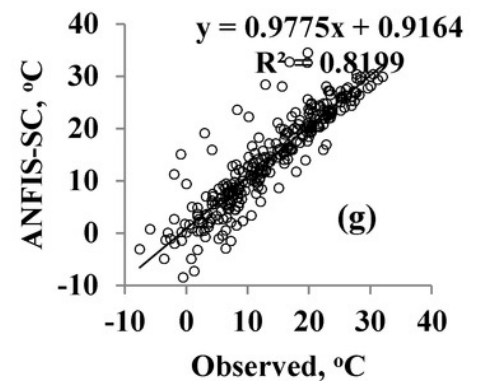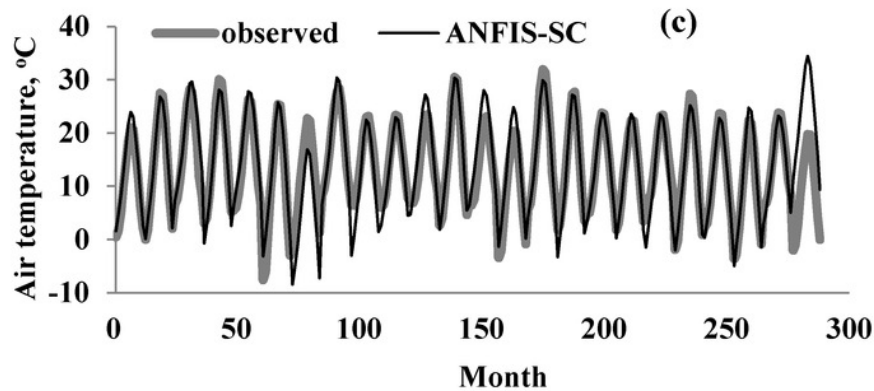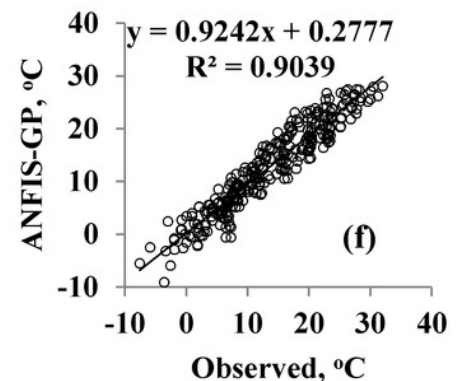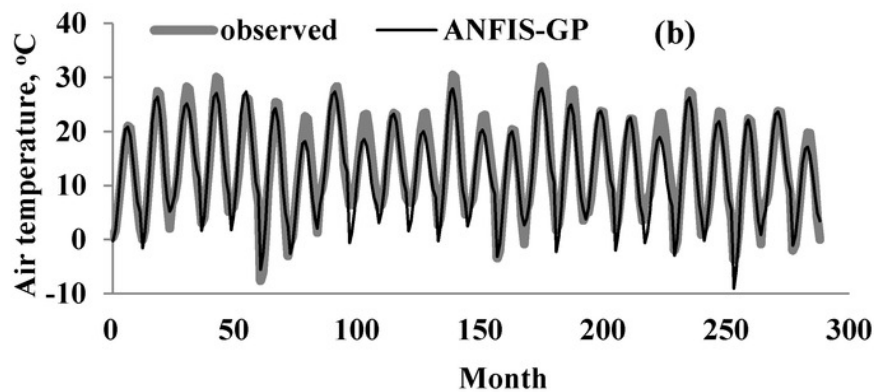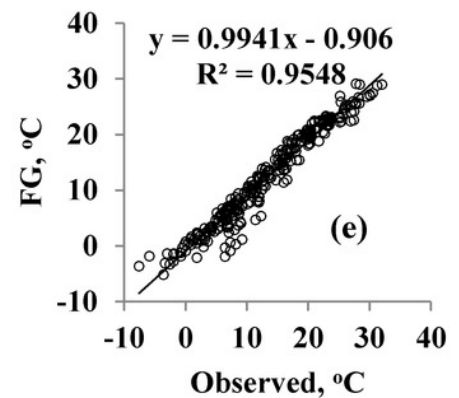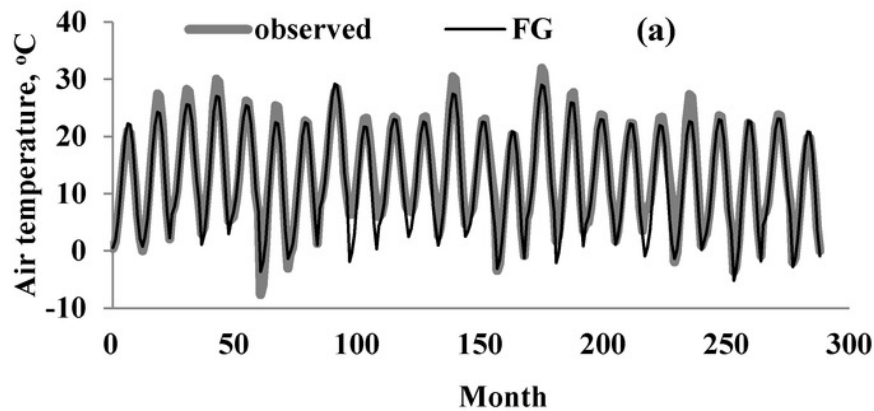
Figure 6

Figure 6.

Observed and predicted air temperatures by FG, ANFIS-GP, ANFIS-SC and ANFIS-FCM models – M2 models; time variation graphs of (a) FG, (b) ANFIS-GP, (c) ANFIS-SC and (d) ANFIS-FCM and scatterplots of (e) FG, (f) ANFIS-GP, (g) ANFIS-SC and (h) ANFIS-FCM
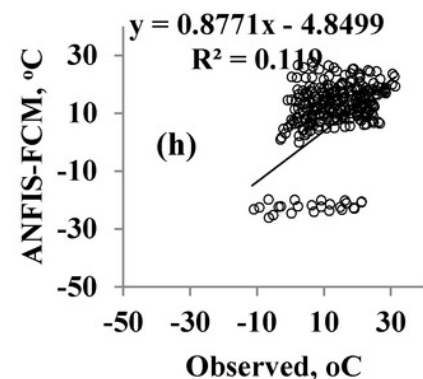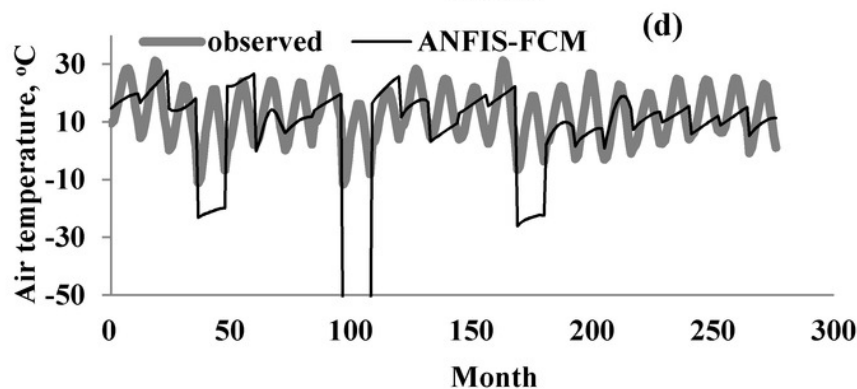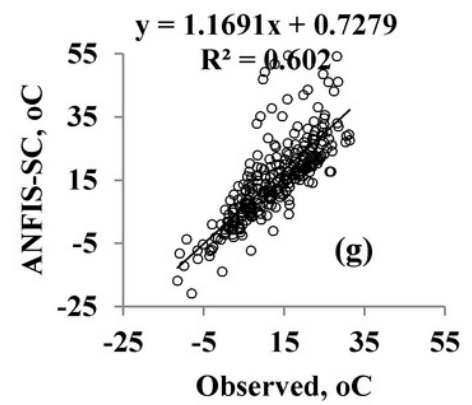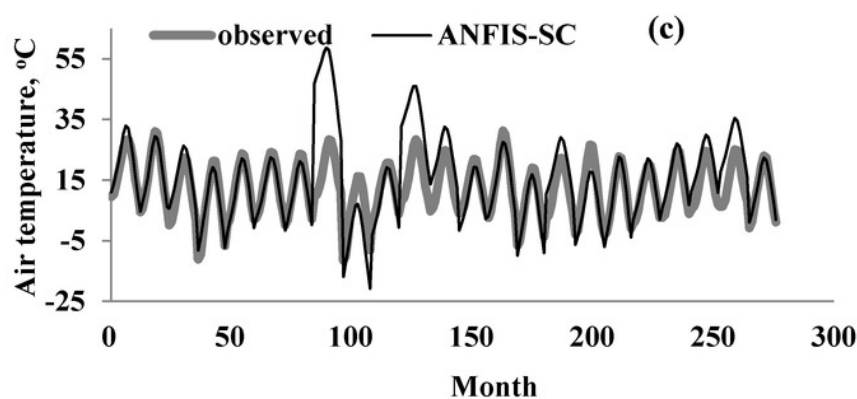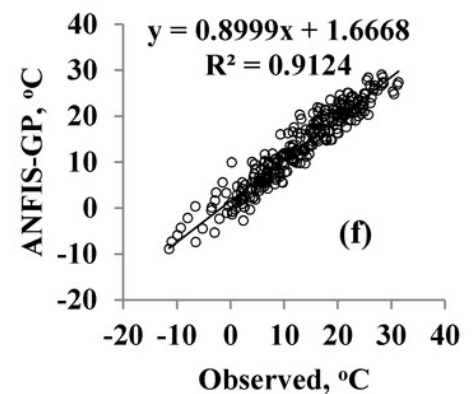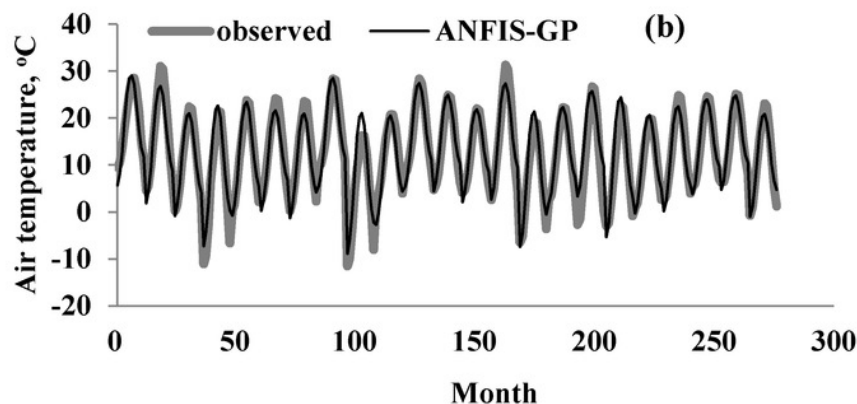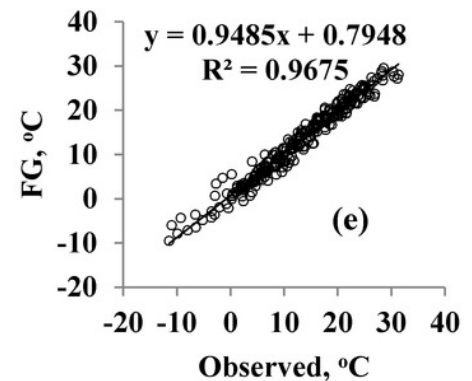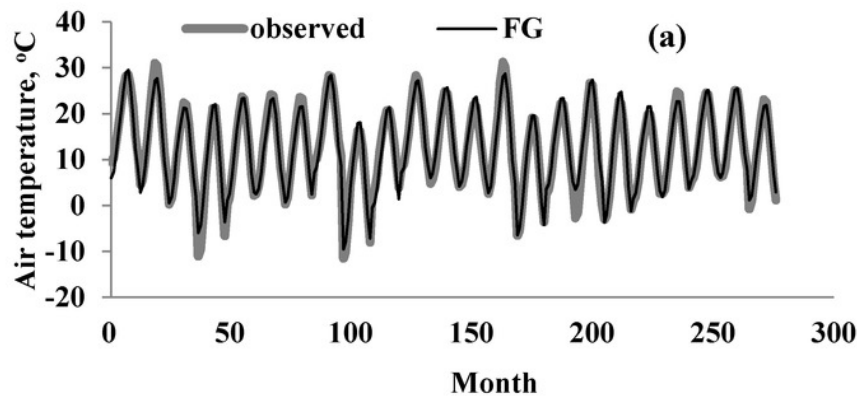
Figure 7

Figure 7.

Observed and predicted air temperatures by FG, ANFIS-GP, ANFIS-SC and ANFIS-FCM models – M3 models; time variation graphs of (a) FG, (b) ANFIS-GP, (c) ANFIS-SC and (d) ANFIS-FCM and scatterplots of (e) FG, (f) ANFIS-GP, (g) ANFIS-SC and (h) ANFIS-FCM
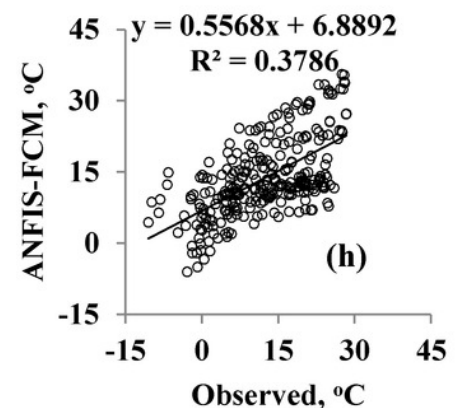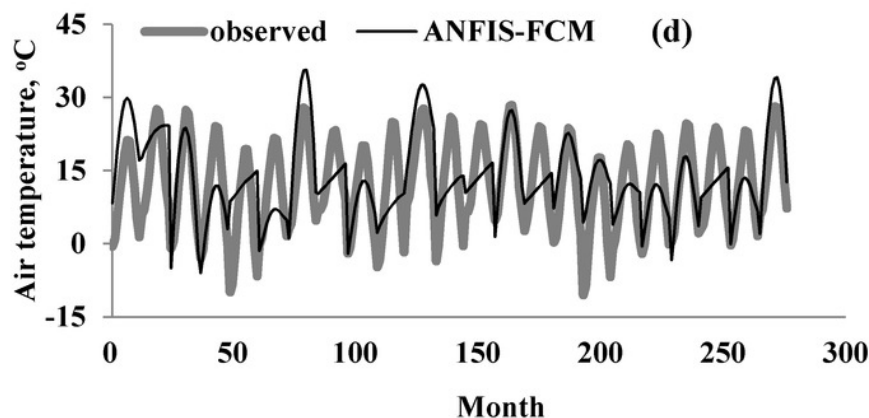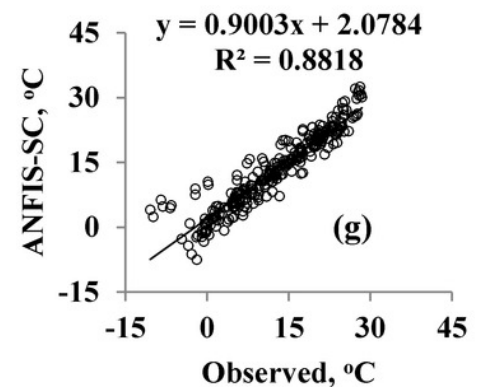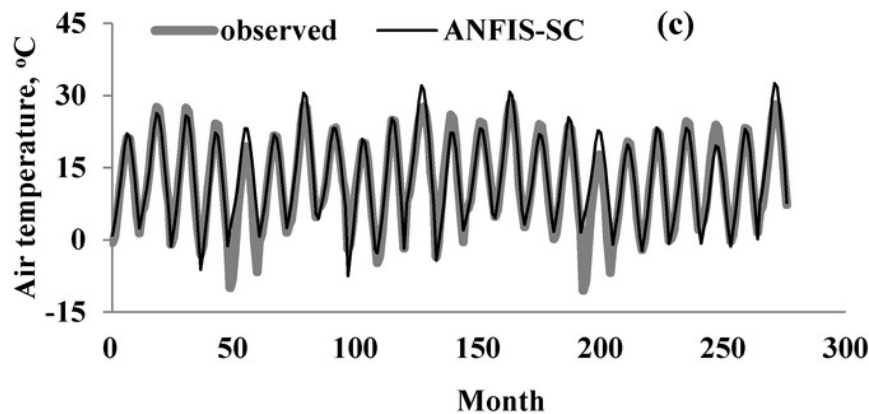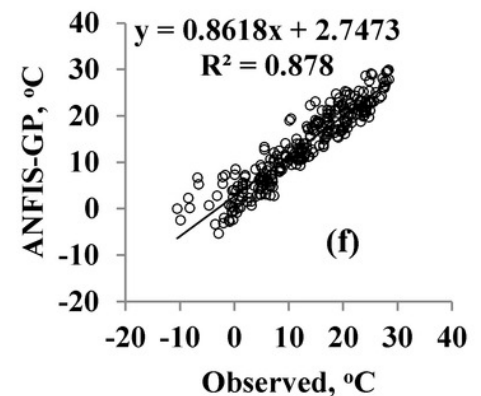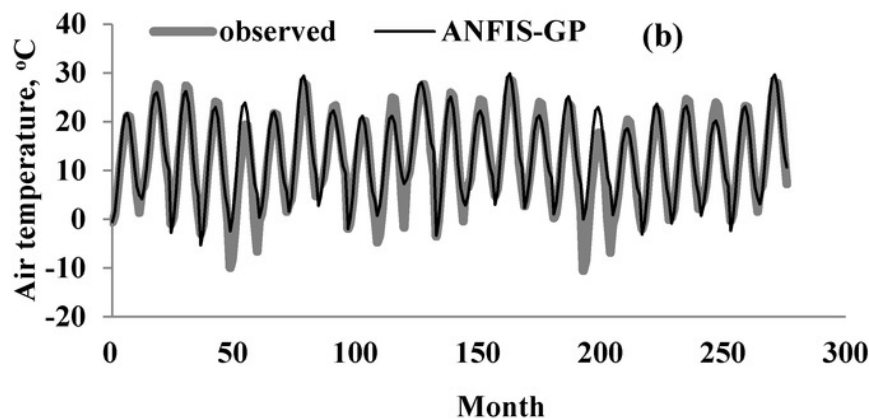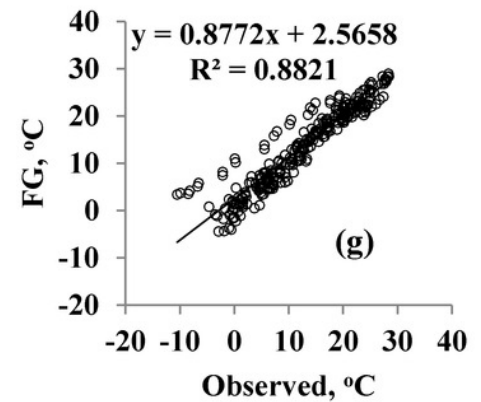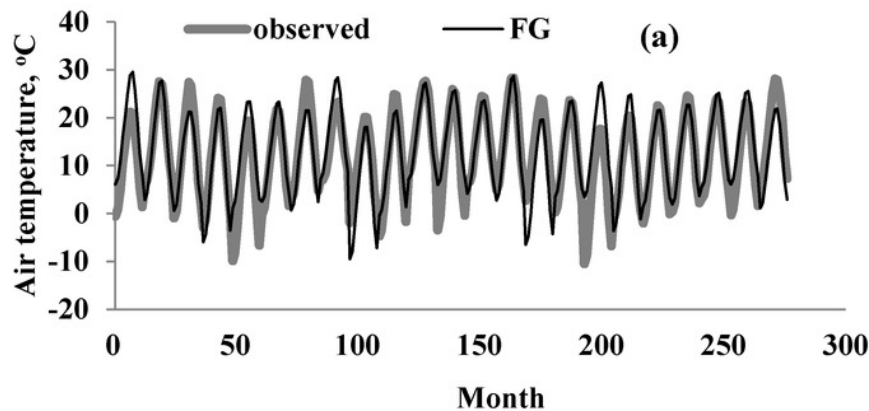
Figure 8

Figure 8.

M1 model output maps for (a) ANFIS-SC, (b) ANFIS-GP, (c) ANFIS-FCM and (d) FG
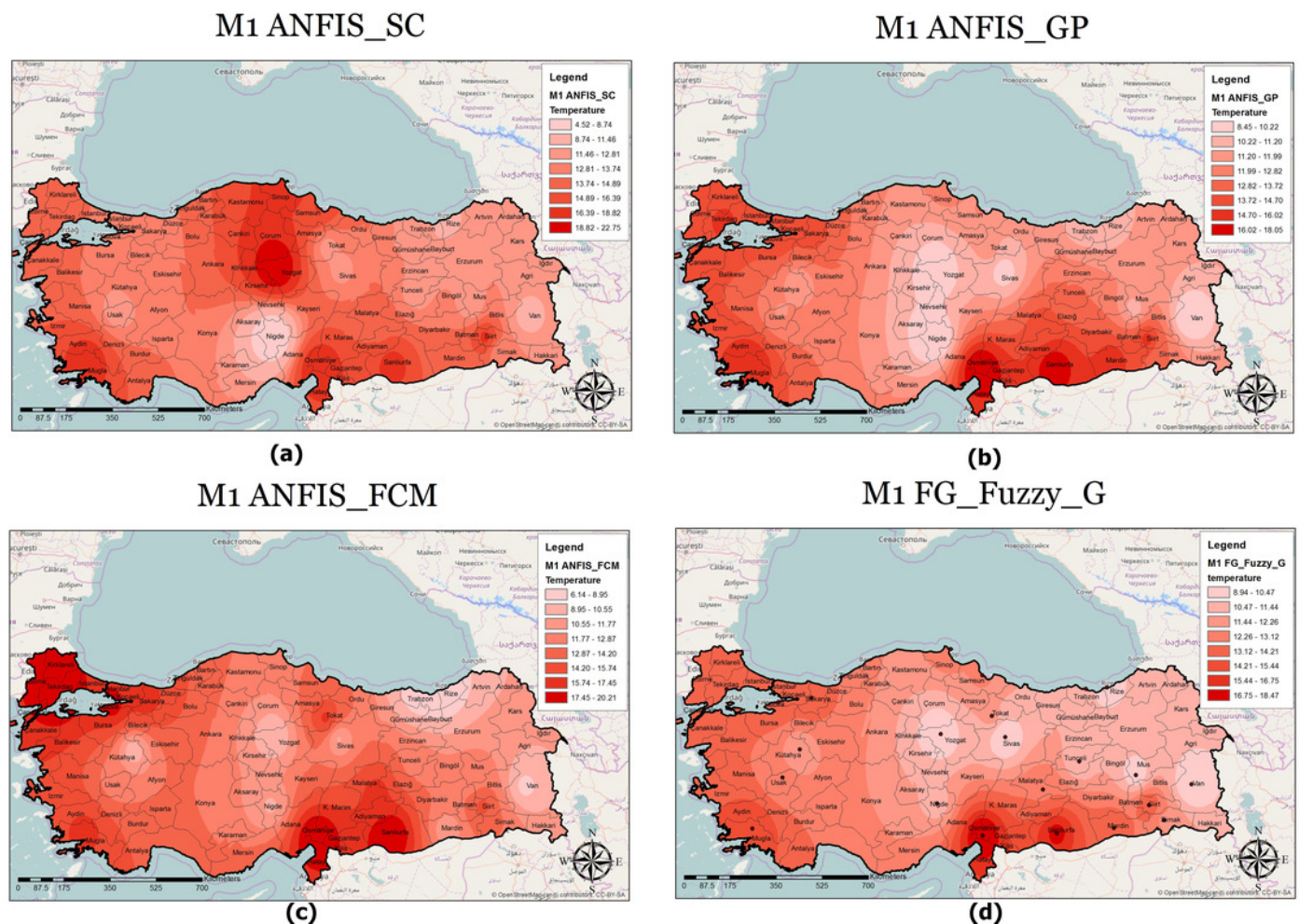
Figure 9

Figure 9.

M2 model output maps for (a) ANFIS-SC, (b) ANFIS-GP, (c) ANFIS-FCM and (d) FG
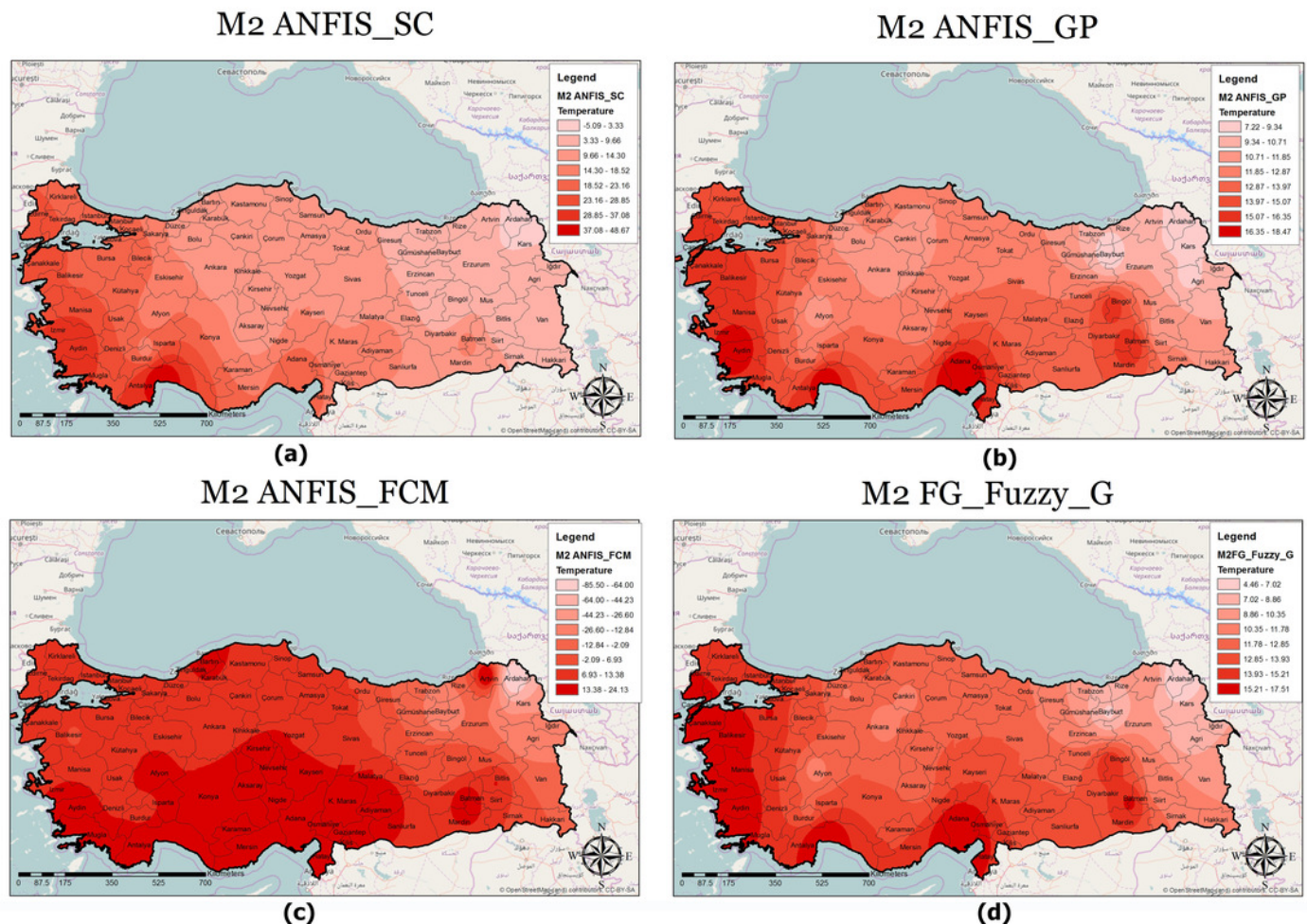
Figure 10

Figure 10.

M3 model output maps for (a) ANFIS-SC, (b) ANFIS-GP, (c) ANFIS-FCM and (d) FG